ELSEVIER International Journal of Mass Spectrometry and Ion Processes 143 (1995) 65–85

International Journal of Mass Spectrometry and Ion Processes

Structural measurements on several alamethicin peptides by the time-of-flight correlation technique

N. Poppe-Schriemer[a,b,*], W. Ens[a], J.D. O'Neil[b], V. Spicer[a], K.G. Standing[a], J.B. Westmore[b], A.A. Yee[b]

[a]*Department of Physics, University of Manitoba, Winnipeg, Man., R3T 2N2 Canada*
[b]*Department of Chemistry, University of Manitoba, Winnipeg, Man., R3T 2N2 Canada*

Received 29 August 1994; accepted 6 October 1994

Abstract

Time-of-flight correlation methods have been used to determine the primary structure of the major component in a nonstandard preparation of alamethicins, and to give some sequence information about minor components. The peptide (MW ≈ 2000 u) is blocked at the N terminus with an acetyl group and has a primary alcohol rather than a carboxyl group at the C terminus, so the usual wet chemical sequencing methods cannot be applied. Upon bombardment with 25 keV I^- ions, the peptide, deposited on the surface of a solid target, produces both molecular ions and prompt fragment ions (i.e. ions formed at or very near the surface of the target). After acceleration, these ions may undergo metastable decay as they pass along the flight tube of a reflecting time-of-flight mass spectrometer. Measurement of the correlations between the neutral and charged daughters from these decompositions determines the decay pattern of each ion, which in turn yields definitive information about the sequence of the original peptide. All events are recorded on magnetic tape and analyzed off-line, so a single run on the spectrometer provides information on the decay of every ion produced at the target, i.e. information similar to that obtainable from a complete set of daughter ion scans on a multiple sector or triple quadrupole instrument.

Keywords: Time of flight; Mass spectrometry; Alamethicin; Metastable decay; Peptide sequencing

1. Introduction

The alamethicins, produced by the fungus *Trichoderma viride*, are members of the peptaibol class of peptides. These are linear, amphiphilic, antibiotic polypeptides (≈ 2000 u) with acetylated N-termini and amino alcohols at the C termini. The peptaibols contain many α-aminoisobutyric acid (Aib) residues and may contain some isovaline residues [1]. Because they are all produced enzymatically (not from an RNA template), amino acid interchanges occur, resulting in whole families of closely related peptides.

The alamethicins can be incorporated into bilayer lipid membranes [2], i.e. membranes consisting of two monolayers, with the hydrophilic sides facing each other. In that condition they induce a conductance that increases with increasing applied voltage [3],

* Corresponding author.

SSDI 0168-1176(94)04116-4

so they are widely used to model voltage-gated ion channels. This behavior is apparently a result of the formation of pores with five discrete voltage-dependent conductance levels [3] in the membrane. Determination of the amino acid sequence of the peptides involved is a first step in understanding the formation and structure of these pores.

Because the compounds are so similar, it is very difficult to separate them completely by HPLC; samples pure enough to crystallize may still not be homogeneous [1,4]. Even if a sample consists of only one peptide, the nature of the peptaibols renders sequencing difficult. As mentioned above, the N terminus is acetylated, so the Edman degradation cannot be used for determining the sequence of amino acids in the peptide, and the C terminus is an alcohol ($-CH_2OH$), ruling out the use of degradations from that end of the peptide. Additional problems are the resistance of the compounds to proteolytic digestion, and the unusual amino acids, namely Aib and perhaps isovaline, that are present. For this reason, mass spectrometry (field desorption, electron impact, and plasma desorption mass spectrometry (PDMS)) has played an important role in determining the primary structure of these compounds [5–7]. Other techniques have also contributed [8,9] and additional information has been provided by gas phase chromatography/mass spectrometry (GC/MS) of a hydrolysate of alamethicins [10]. Tandem mass spectrometry has been applied to other peptaibols, the trichosporin compounds for example [11], but not to the alamethicins themselves.

The amino acid sequences of the two main alamethicin components (I and II) grown under standard (Upjohn) conditions [12] (Fig. 1b) are thus known. The sequence of alamethicin I is [6]

$$Ac\text{–}Aib_1\text{–}Pro_2\text{–}Aib_3\text{–}Ala_4\text{–}Aib_5\text{–}Ala_6\text{–}Gln_7\text{–}Aib_8\text{–}Val_9\text{–}Aib_{10}\text{–}Gly_{11}\text{–}Leu_{12}\text{–}Aib_{13}\text{–}Pro_{14}\text{–}Val_{15}\text{–}Aib_{16}\text{–}Aib_{17}\text{–}Glu_{18}\text{–}Gln_{19}\text{–}Phe_{20}\text{–ol} \quad (1)$$

Alamethicin II differs from this only by the replacement of Ala by Aib in position 6 [6]. As well, the GC/MS study indicated that Aib-Ala interchanges may occur at residues 4, 5 and 6, and that Aib–Val interchanges may occur at residues 9, 16 and 17 [10]. Several different families of fungal antibiotics that are very similar to the alamethicins have also been analyzed by mass spectrometry [1,4,11,13], with similar results.

However, even mass spectrometric sequencing is not trivial. Most peptaibols contain at least one Aib-Pro bond (usually between positions 13 and 14), which is very easily fragmented in fast atom bombardment (FAB) mass spectrometry [11,13]. Fragmentation in collisionally induced dissociation (CID) also occurs preferentially at Pro [13(a)]. As a result, the mass spectrum is very complicated, with most spectral peaks in the low mass region; generally two or three acylium ion series are present. It turns out to be relatively simple to sequence the first 13 or so residues, but the remainder of the peptide, from the Aib_{13}–Pro_{14} bond to the C-terminus, is significantly more difficult.

It has been noted that "...chemical treatment, such as partial hydrolysis or NMR measurements must be performed in order to confirm the peptide sequences" [11]. One method used involves acid hydrolysis of the Aib–Pro bond. When the resulting hydrolysis mixture is examined by FAB using a glycerol matrix, the prolylheptapeptaibol product gives the most abundant peak, and its sequence specific fragment ion peaks are also abundant, allowing the remainder of the peptide to be determined [13].

The amount of each alamethicin peptide produced is sensitive to the environment in which the fungus is grown [14]. A method for preparing the alamethicins [14] differing from the standard (Upjohn) one has recently been applied in one of our laboratories [15]. High performance liquid chromatography (HPLC) of the resultant peptide mixture exhibits an

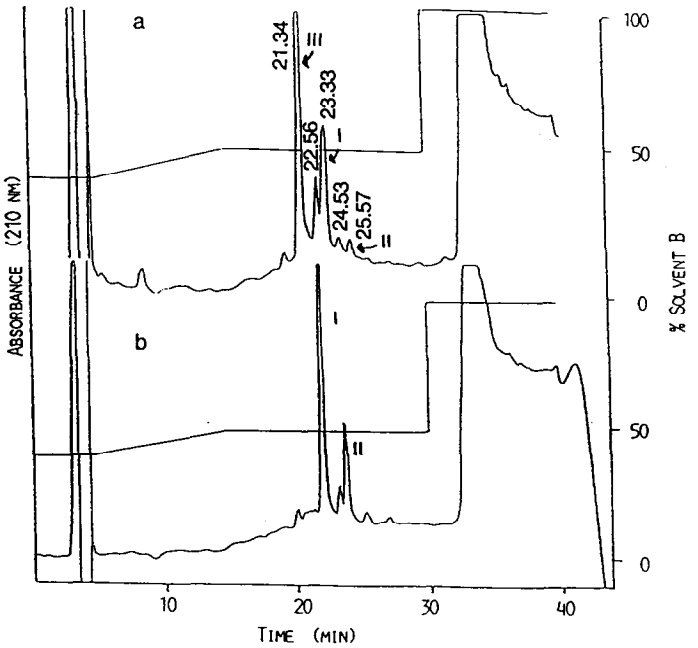

Fig. 1. HPLC of crude alamethicin preparations: (a) Yee and O'Neil preparation [15] used here (peak elution times are given in minutes); (b) the standard alamethicin preparation (Upjohn) method [12]). Samples of 100–500 μl were loaded onto a Beckman Spherisorb 5 μm C-18 reverse-phase column (10 mm i.d., 150 mm length). Solvent A is 0.05 N acetic acid adjusted to pH 3.5 with triethylamine. Solvent B is tetrahydrofuran/acetonitrile/solvent A (8:2:1). Isocratic elution (40% solvent B) at 1 ml min^{-1} for 5 min, was followed by a gradient elution at 1.5 ml min^{-1} for 10 min to 49% solvent B, then by isocratic elution at ml min^{-1} for 15 min, and finally by elution at 1 ml min^{-1} for 10 min at 100% solvent B [15]. (Note that the elution times differ slightly for the two chromatograms.)

abundant component (denoted III in Fig. 1a) not prominent in the standard preparation, as well as some others. These other components include the two main peaks produced by the standard preparation, but there also appear to be additional compounds, as yet uncharacterized. Our measurements indicate that some of the chromatographic peaks consist of more than one component, so the situation is even more complicated than it appears.

It might be expected that the structure of this major component, which we call alamethicin III, is similar to that of the two known components, I and II, whose chromatogram is show in Fig. 1. It has been examined by Yee and O'Neil using NMR spectrometry [15]. Their results are consistent with the same sequence as for alamethicin I above, except for the substitution of Gln for Glu at position 18. However, the NMR measurement required 1 μmol (2 mg) of sample, and insufficient material was available to make NMR measurements on the less abundant components.

Here we describe the detailed sequence verification of alamethicin III using the correlation method developed by the Orsay group [16] and ourselves [17–19] for use in reflecting time-of-flight (TOF) spectrometers. Some results on the other alamethicins are also reported. Noteworthy features of the alamethicin mass spectra are compared to the results obtained earlier for closely related peptide antibiotics.

Our previous investigations of peptide ions which undergo decay, using this correlation method [18,20–24], dealt with fairly simple cases, where the decays of only a few parent ions were examined. However, we believe that the real strength of the technique lies in its

ability to examine the decays of many parent ions at the same time, and thus to examine a given daughter ion produced by several different parents; this provides additional confidence in the deduced structure. In addition, it may be of some interest to obtain the metastable decay pattern of a whole series of similar ion types, such as the series of prompt alamethicin III fragment ions observed here, corresponding to successive deletions of a single amino acid residue. Because most of the prompt fragment ions of the alamethicins show metastable decay and because many of its HPLC fractions contain more than one peptide, the present work serves as a test of the utility of the technique in a fairly complicated case. Moreover, the conclusions can be tested by comparison with the result of the NMR measurements mentioned above and with mass spectral results for closely related peptaibols.

2. Experimental method

Alamethicin III was separated from the crude alamethicin mixture by reversed phase HPLC, as described in the caption to Fig. 1. A fraction collected from the central part of the largest peak (21.34 min, denoted III in Fig. 1a) was recrystallized to remove impurities, then dissolved in 0.1% trifluoroacetic acid, and deposited on to electrosprayed nitrocellulose. An estimated 5 nmol were deposited on each target used; the collected fraction yielded sufficient material after recrystallization so that no particular effort was necessary to conserve sample. This rather large amount was used for convenience; previous measurements have shown that complete sequence information can be obtained on 200 fmol of peptide with our technique [24,24(a)]. The other HPLC fractions examined were treated like alamethicin III, except that they were not recrystallized.

The measurements were carried out on our reflecting TOF mass spectrometer, TOF II [19] (Fig. 2). Secondary ions were formed by bombardment of the solid sample target by I^- primary ions at 25 keV [25]; the I^- ions gained an energy of 15 keV in the ion gun and 10 keV from the secondary ion voltage. (When positive secondary ion spectra were being examined, the use of negative primary ions was an advantage, since the 10 kV secondary ion acceleration voltage accelerated them also.) In the few cases where negative ions were examined, the incident I^- ions were slowed to an energy of 5 keV by the −10 kV secondary ion accelerating voltage.

Ion bombardment produces a variety of charged molecules and fragment ions from the peptide at (or very near) the surface of the solid target. We shall refer to these fragments as "prompt" fragment ions. Both

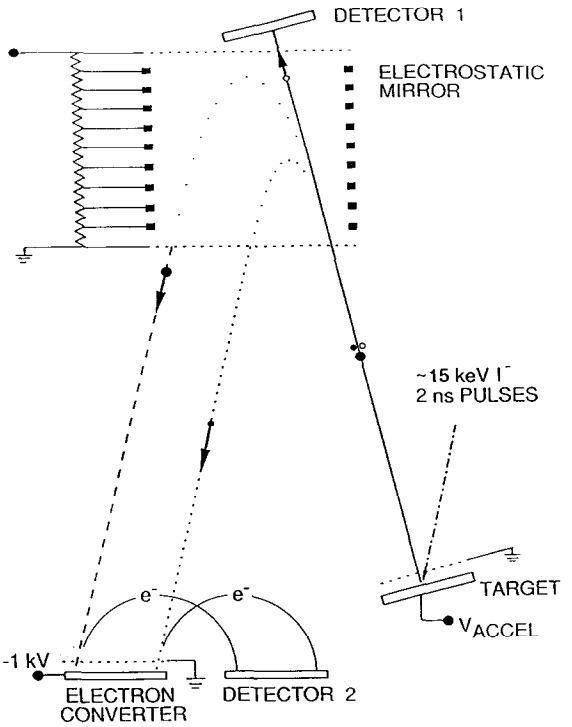

Fig. 2. TOF II, the reflecting time-of-flight secondary ion mass spectrometer used in this work.

molecular ions and prompt fragment ions are accelerated to an energy of 10 keV and they (or their decay products) are detected either at the end of the flight tube or after reflection in the mirror.

In the simplest mode of operation of the spectrometer, there is no field in the electrostatic mirror, so the TOF spectrum (the "direct spectrum") is observed in detector 1 (Fig. 2) and the device operates as a linear TOF spectrometer. If the molecular ions or the prompt fragment ions decay as they pass along the flight tube, their neutral and charged daughters continue with approximately the same velocity as their respective parent ions. Therefore the daughters appear as a broadened peak at the same position as the parent ion peak.

When the spectrometer is operated in the reflecting mode, the voltage on the mirror is normally set to a value that optimizes the resolution for the parent ions [19]. Under these conditions, ions that reach the mirror without decaying (both molecular ions and prompt charged fragments) are reflected by the mirror and observed with improved resolution in detector 2. If an ion decays in free flight between the target and the mirror, the neutral daughter, which is not affected by the mirror, continues to detector 1 where its measured flight time serves to identify its parent. The charged daughter is reflected into detector 2, where its mass is determined by the ratio of its flight time to the flight time of its parent [19]. Observation of the correlations between charged and neutral daughters then enables one to determine the decay of each parent ion, i.e. the decays of both the molecular ion and the prompt fragment ions [16–19].

To record this complex array of data it is essential to have an efficient data system [26]. Here the system is controlled by an Atari TT030 microcomputer, which uses a 68030 microprocessor running at 32 MHz (Fig. 3). The Orsay model CTN/M2 time-to-digital converter (TDC) is connected to the VME bus of the computer with a custom interface, designed and constructed in our laboratory. This TDC has one common input (for the start signal) and three individually coded stop inputs, of which two are used here. For each primary ion pulse, the TDC receives a start signal from the ion gun clock in the common input. If events are measured in detector 1 or 2, the TDC generates an individually coded stop signal for each event. For each primary ion pulse the stop times are grouped together with their start time in a 512 byte buffer. The TT030 polls the TDC 60 times a second for data from the common start and the two stops. Flight times from detector 1, occurring within a particular time window, will trigger storage of the corresponding flight times from detector 2 as a histogram into a reserved area of computer memory; a correlated spectrum is then constructed from the stored information.

In our previous correlation measurements, the spectra were recorded in real time during the spectrometer run [17,18,20–24,27]. However, this method requires a trial run to determine the time windows for the detection of neutrals, and the measurement may have to be repeated if any mistakes are made in setting the windows. Also, the method requires a good deal of memory, and several experiments may be necessary if many correlated spectra are to be recorded. For these reasons, we have developed an alternative procedure for the experiments reported here; the flight times are recorded directly onto magnetic tape, event by event, instead of sorting then into histograms on line. Thus, the experiment may be "replayed" later with the taped data substituting for those normally coming directly from the spectrometer's detector. As many as ten correlation spectra can be recorded simultaneously in such a "replayed" experiment. Furthermore, this can be done in

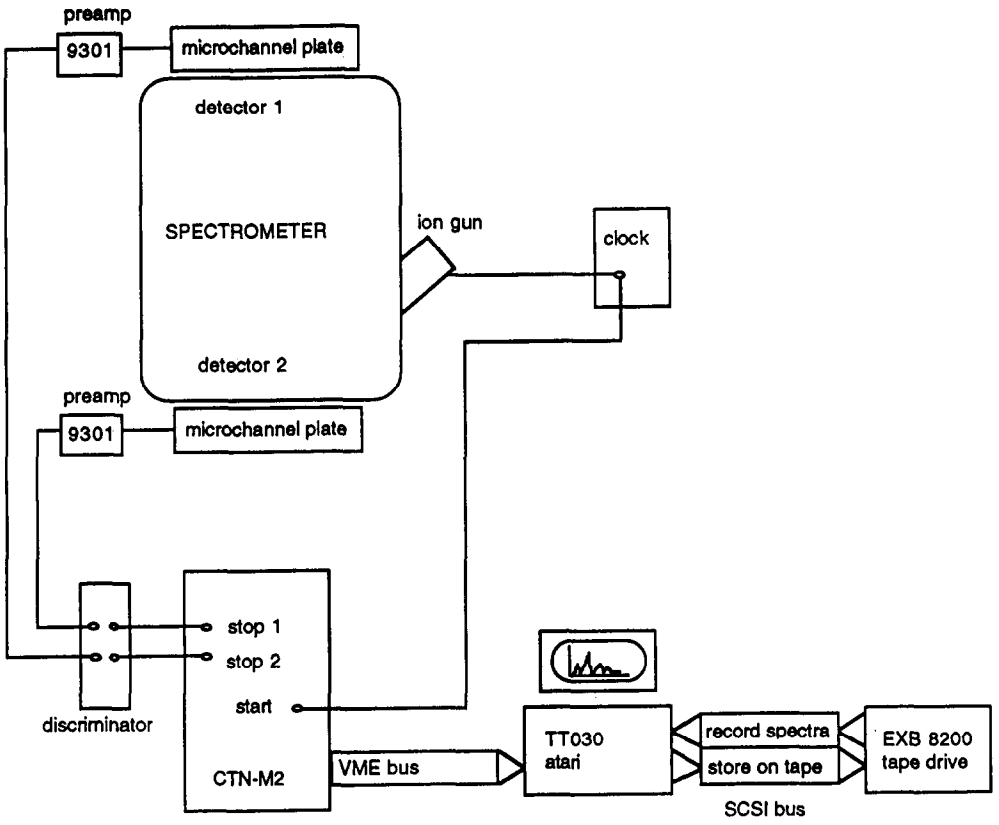

Fig. 3. Schematic of the datalogging system.

less time than the actual spectrometer experiment because the restrictions on counting rate imposed by the instrument and the data system no longer apply. Because multiple replays of a run allow extraction of a daughter ion spectrum from every ion that decays, the sensitivity of the experiments is greatly increased. Also flexibility is considerably improved; the effect of changes in the time window can be investigated easily by replaying the tape with new window settings. Although a spectrometer run is typically about 4–5 h, the data can be "replayed" from the tape in about 75% of the time.

For this procedure an Exabyte EXB-8200 8 mm tape drive is connected to the TT030 through its SCSI port. Each 8 mm tape can store up to 2 gigabytes of data corresponding to about 15 h of acquisition time. The acquisition software writes blocks of raw neutral and ion flight times on to tape at a maximum rate of about 17 000 events per second (events include both stop and start signals).

3. Results

3.1. Direct and neutral spectra

As pointed out previously [28], bombardment of a solid target by primary ions at kiloelectronvolt energies yields a variety of secondary ions at the target surface very similar to those produced by collisional activation of ions in a gas cell at similar energies. In particular, side-chain fragmentations [29] are

often observed [28], enabling leucine and isoleucine to be distinguished. In both methods continuous (or semicontinuous) sequences of one or more fragment ion species are normally produced, but in some cases our technique appears to be even more informative. For example, we were able to obtain considerable sequence information on the peptide dynorphin A, which has a large number of basic residues (five) in the central region of the molecule [28,30]. By comparison, an extensive investigation of the compound by tandem mass spectrometry, using both high energy CID of ions produced by LSIMS and low energy CID of electrosprayed ions, failed to yield any coherent series of fragments [31].

In the present case most of the prominent ions in the direct spectrum (Fig. 4a) can be assigned to the series B_1 to B_{13} (using the accepted notation, Fig. 5). The $Y_7 + 2$ ion, several A_n or D_n ions, and several $Y_{19}B_n + 1$ ions are also abundant. The same ion species are seen in the strong neutral spectrum (Fig. 4b), which arises from metastable decay in the first leg of the flight path. The peaks in these spectra are quite broad, e.g. about 190 ns for the $(M + H)^+$ ion corresponding to a mass resolution $M/\Delta M_{FWHM} \approx 75$, consistent with

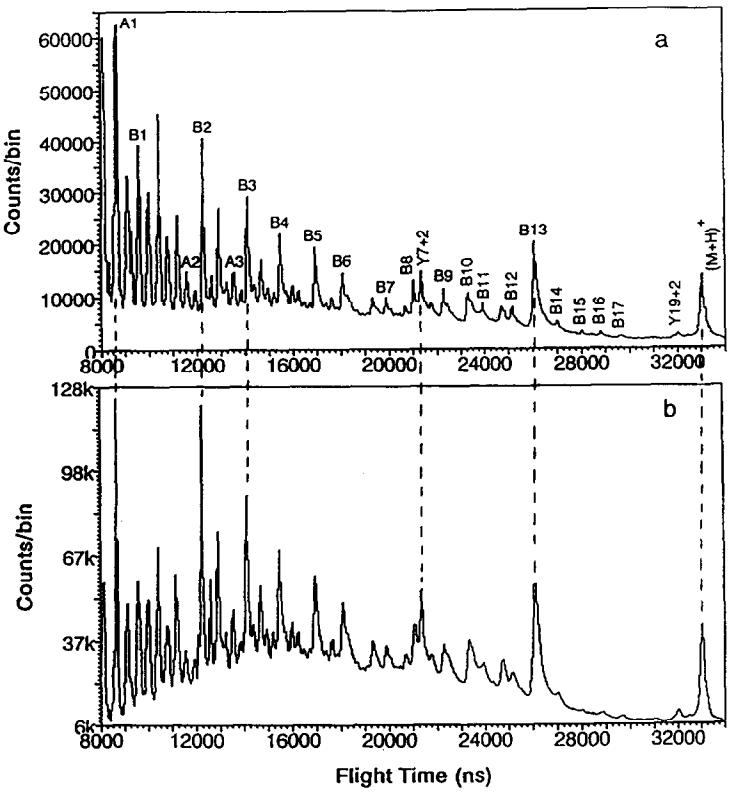

Fig. 4. (a) "Direct" spectrum of alamethicin III observed in detector 1 with zero voltage on the mirror. Masses of the fragment ions, calculated using an in-house program (JBW) as well as MacBioSpec (Sciex), were used to make the assignments shown (in the standard notation [32,33]). The sequence given in Eq. (1), with Gln_{18} substituted for Glu_{18}, was assumed. (b) "Neutral" spectrum of alamethicin III observed in detector 1 when a reflecting voltage was applied to the mirror. Broken lines are drawn between several of the corresponding peaks in the direct and neutral spectra to emphasize their identities. The many large neutral peaks indicate a good deal of metastable decay. (Note that the acquisition times differ for the two spectra.)

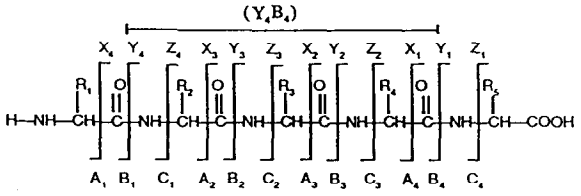

Fig. 5. Fragment ion patterns and notation [32,33]. Extra hydrogen atoms in an ion are denoted by "+1" or "+2".

previous results [27]. The peak width is determined mainly by the spread in velocity of the daughters produced by metastable decay; this results from the finite energy release in the disintegration.

As mentioned above, the flight time of a neutral daughter serves to identify its parent, i.e. a molecular ion or a "prompt fragment". A "prompt fragment" can of course be produced directly at the target by the primary ion impact. In addition, however, the fragment may itself be a product of the decay of a larger ion close to the target, as discussed in Appendix 1. For example, the B_{13} "prompt fragment" peak in the neutral spectrum defines B_{13} ions that are produced within about 100 ns after impact, and that subsequently decay in free flight. The low intensity of the B_n series ions beyond B_{13} indicates that any such ions produced at the target have lifetimes $\lesssim 100$ ns.

3.2. Reflected spectrum

For most compounds, one could expect to see the same ion species in the reflected spectrum as in the direct spectrum, but with better resolution. In this case, however, the ions from alamethicin III were found to undergo an unusual amount of decomposition along the flight path. This facilitated the correlation measurements, described later, but made it difficult to extract much information from the reflected spectrum (Fig. 6) [30]. In particular, the $[M + H]^+$ ion peak is barely visible at about 1963 u in the molecular ion region, as shown in Fig. 7. Fortunately, the $[M + Na]^+$ ions are more stable and give a prominent peak; the principal mass is measured as 1985.1 u. The $[M + Na]^+$ assignment was confirmed by observation of the $[M - H]^-$ ion at 1961.3 u in the negative ion spectrum. The measured mass of the peptide is then 1962.1 u i.e. 1 u less than that of alamethicin I, consistent with the proposed replacement of Glu_{18} by Gln_{18}.

Thus the overall mass measurement, as well as the NMR result mentioned above, is consistent with the sequence given in Eq. (1), with the substitution of Gln_{18} for Glu_{18}. The assignments of Fig. 4a were made after comparing the observed fragment masses with those calculated from this structure. The agreement between observed and calculated values lends the sequence considerable support, at least for the first 13 residues. The very small peaks assigned as B_{14} to B_{19} (excluding B_{18}) are consistent with expectation, but are much less definitive, so little information is available on residues 14 to 19. Also, the limited accuracy of mass determination (± 0.5 u at low mass to ± 2 u at high mass) due to the wide peaks, leaves some ambiguities. Even though the residue masses are derived from differences between the peaks, not from their absolute masses, the assignments Gln/Lys/Glu, Aib/Ser, Leu/Ile and Val/Pro/Thr cannot always be distinguished.

Other arguments can be used to reduce the uncertainties. In particular we note that the $Y_7 + 2$ ion is the only large C-terminal fragment observed and the complementary B_{13} fragment is prominent. Both of these correspond to cleavage at Aib_{13}–Pro_{14}, and give strong support to that assignment, since the Aib–Pro bond is known to cleave preferentially [11,13]. However, it is clear that more information is still required to define the sequence, certainly for residues beyond 14.

3.3. Correlation spectra

As discussed above, primary ion bombard-

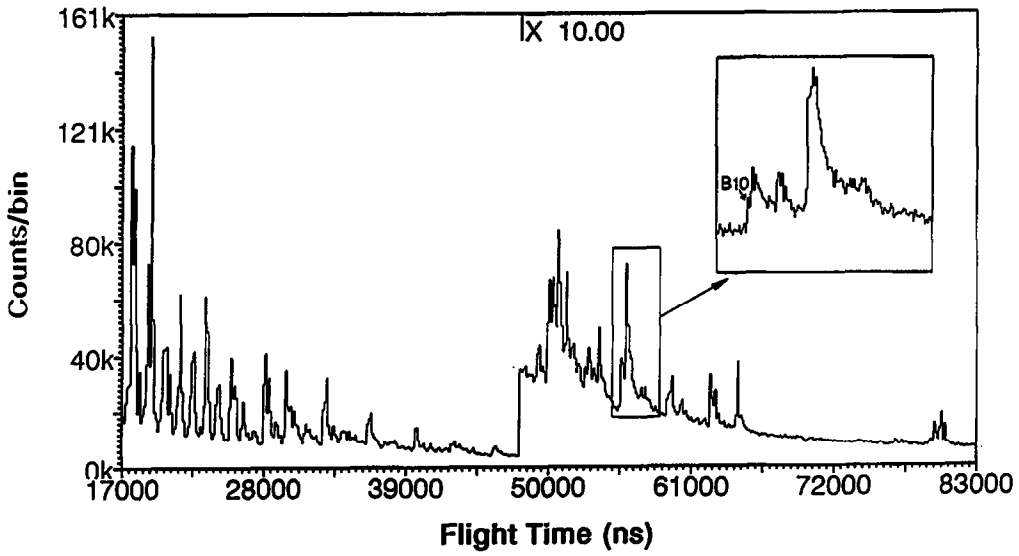

Fig. 6. A portion of a reflected spectrum showing near overlap between prompt B_{10} ions and the daughter B_{10} ions arising from metastable decay of heavier ions, such as B_{11}, B_{12}, B_{13} and $[M + H]^+$. The prompt B_{10} ion is the tiny peak labeled in the insert, and the daughter B_{10} ions appear to its right [30].

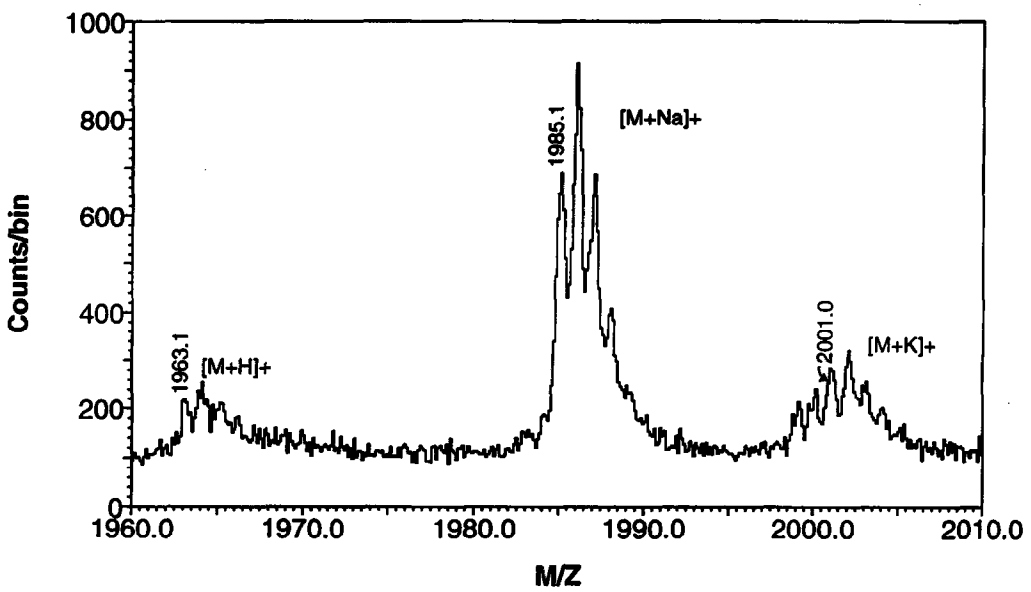

Fig. 7. The molecular ion region of a reflected spectrum of alamethicin III. The principal mass of $(M + Na)^+$ was measured to be 1985.1 u on the basis of a calibration with the H^+ and $C_3H_3^+$ ions, which has been found to give masses accurate to ≈ 0.1 u for peptides as large as 2000 u in previous measurements [24]. A calibration using H^+ and [substance P + H]$^+$ gave identical results. The small cluster of peaks at 2001 u corresponds to $[M + K]^+$. The $[M + Na]^+$ peak at 1986.1 u is larger than expected, consistent with the presence of an impurity of that mass, probably alamethicin I. The peaks at 1999 u, interfering with the $[M + K]^+$ peaks, suggest the presence of another impurity. Rechromatographing the sample under the conditions previously used showed that it did, in fact, contain two impurities, consistent with this interpretation.

ment produces a variety of secondary ions at the target, both molecular ions and prompt fragment ions. If the ion survives acceleration but subsequently decays before it enters the mirror, the flight time of the neutral daughter (observed in detector 1) defines the parent ion. The parent ion can itself be the product of the decay of a precursor close to the target. What the neutral spectrum actually measures is the parent ion distribution that exists about 100 ns after desorption, as discussed in Appendix 1.

However, the time of arrival of the correlated daughter ion at detector 2 measures the daughter ion spectrum at the entrance to the mirror, i.e. about 10 μs after the desorption event. Thus the technique measures decays of the parent ion that occur during the time they travel from the acceleration grid to the mirror, $\approx 0.5\,\mu$s to $\approx 10\,\mu$s after desorption.

The correlation spectrum for the decay of the $[M + H]^+$ ion is shown in Fig. 8 and representative spectra for several of the prompt fragment ions in Figs. 9 and 10. The decay products from the B ions are summarized in Table 1.

(*a*) *Decay of* $[M + H]^+$

The $[M + H]^+$ ion produces mainly B_8, B_9, B_{10}, B_{13} and $Y_7 + 2$ ions (Fig. 8) as well as several smaller peaks. The absence of B_{14} to B_{19} and the prominence of the complementary ions B_{13} and $Y_7 + 2$ are consistent with the data shown in the direct spectrum; again cleavage at Aib_{13}–Pro_{14} is preferred. The smaller peaks correspond to the remaining B_n ions and to internal fragments, $Y_{19}B_n + 1$, with cleavage at the other Aib–Pro bond (Aib_1–Pro_2).

(*b*) *Decay of* B_n

Many of the B_n ions ($n = 3$–14 and 19) decay into lower mass B_m ions by loss of one or more residues from the C terminus, e.g. the daughters of B_{13} include ions from B_3 to B_{11} (Table 1). (If the B_{13} ion originated from decay

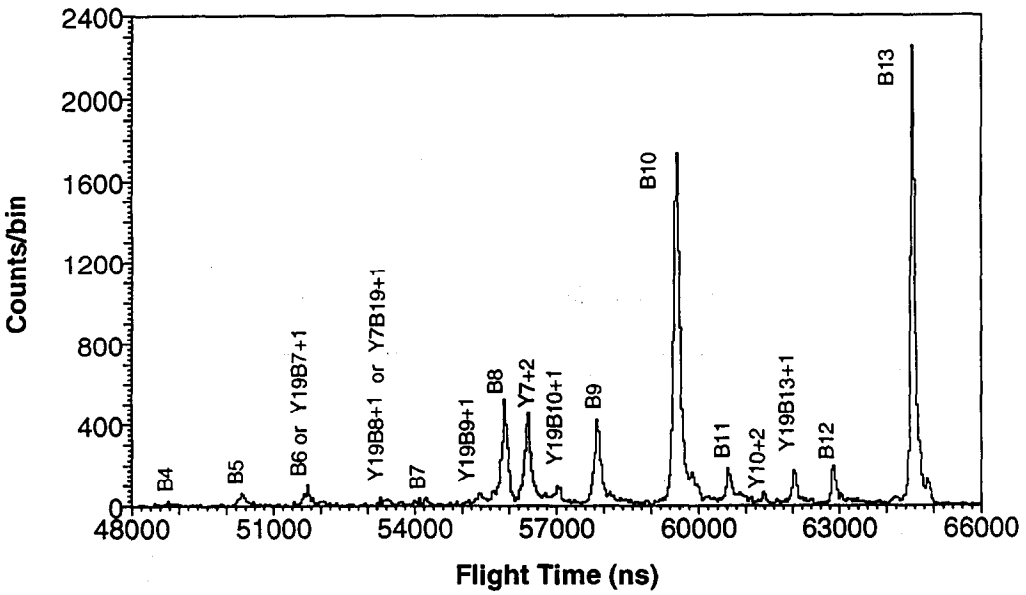

Fig. 8. Daughter ion spectrum of $[M + H]^+$ parent ions.

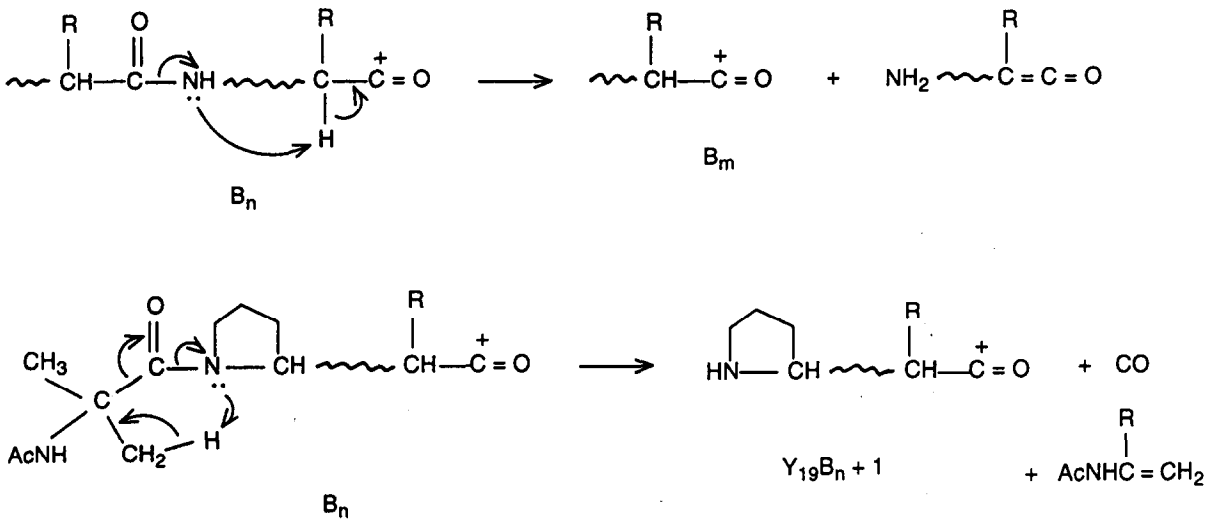

Scheme 1. Decompositions of B_n.

of an $[M + H]^+$ ion near the target, these ions would then be granddaughters of the original $[M + H]^+$ ion). Values of m for daughters of a given B_n ion are shown in Table 1. These cleavages are sometimes accompanied by a cleavage at Aib_1–Pro_2 (as for $[M + H]^+$) to produce internal fragment ions beginning with Pro_2 (i.e. $Y_{19}B_n + 1$), perhaps as depicted in Scheme 1. As representative examples, daughter ion spectra for B_7 to B_9 are shown in Fig. 9. The smaller B_n decay to A_n (or D_n) ions as well. The B_1 ion decays into an acetyl ion (m/z 43), the Aib immonium ion, and others, confirming the N-terminus as Ac–Aib.

Decays of several $Y_{19}B_n + 1$ ions (B_n ions less the N-terminal Ac–Aib_1) were also examined. Like the B_n ions, these ions decay into a series of fragment ions containing the C or N termini of their parents, as well as internal fragments.

These decays confirm nearly the whole sequence from the N terminus to B_{13}, with discrepancies in mass of $\lesssim 0.6$ u. However, the $(Leu/Ile)_{12}$ ambiguity was not resolved because of overlap between the diagnostic D_n ions and other ions. Leu_{12} seems more likely because of its presence in the alamethicin I and II sequences.

(c) *Decay of* $Y_7 + 2$

Although they contain much information about the first 13 residues, none of the decay patterns discussed above provide information about the sequence from amino acid 14 to the C terminus, except for the decay of the $[M + H]^+$ ion to a $Y_7 + 2$ ion, which confirms that this ion has approximately the expected mass.

In principle, the decay of the $Y_7 + 2$ ion defines the rest of the sequence, since the daughters include $Y_7B_n + 1$ ions with $n = 15$–19 as shown in Fig. 10. The differences between these peaks have errors of about 1 u; they determine the sequence as $-(Aib/Ser)_{16}$–Aib_{17}–$(Gln/Lys)_{18}$–$(Gln/Lys)_{19}$–Phe_{20}–ol.

This measurement found residue 18 to be Gln/Lys, but we thought it desirable to verify the assignments more precisely, since it is the only change expected from the sequence of alamethicin I. In addition, there were indications of some Glu impurity (see below). Therefore we carried out measurements in which the mirror voltage was successively optimized for the $Y_7B_{17} + 1$ ion and the $Y_7B_{18} + 1$ ion, thus bracketing residue 18. This is carried out by reducing the mirror voltage until the flight time of the desired daughter ion

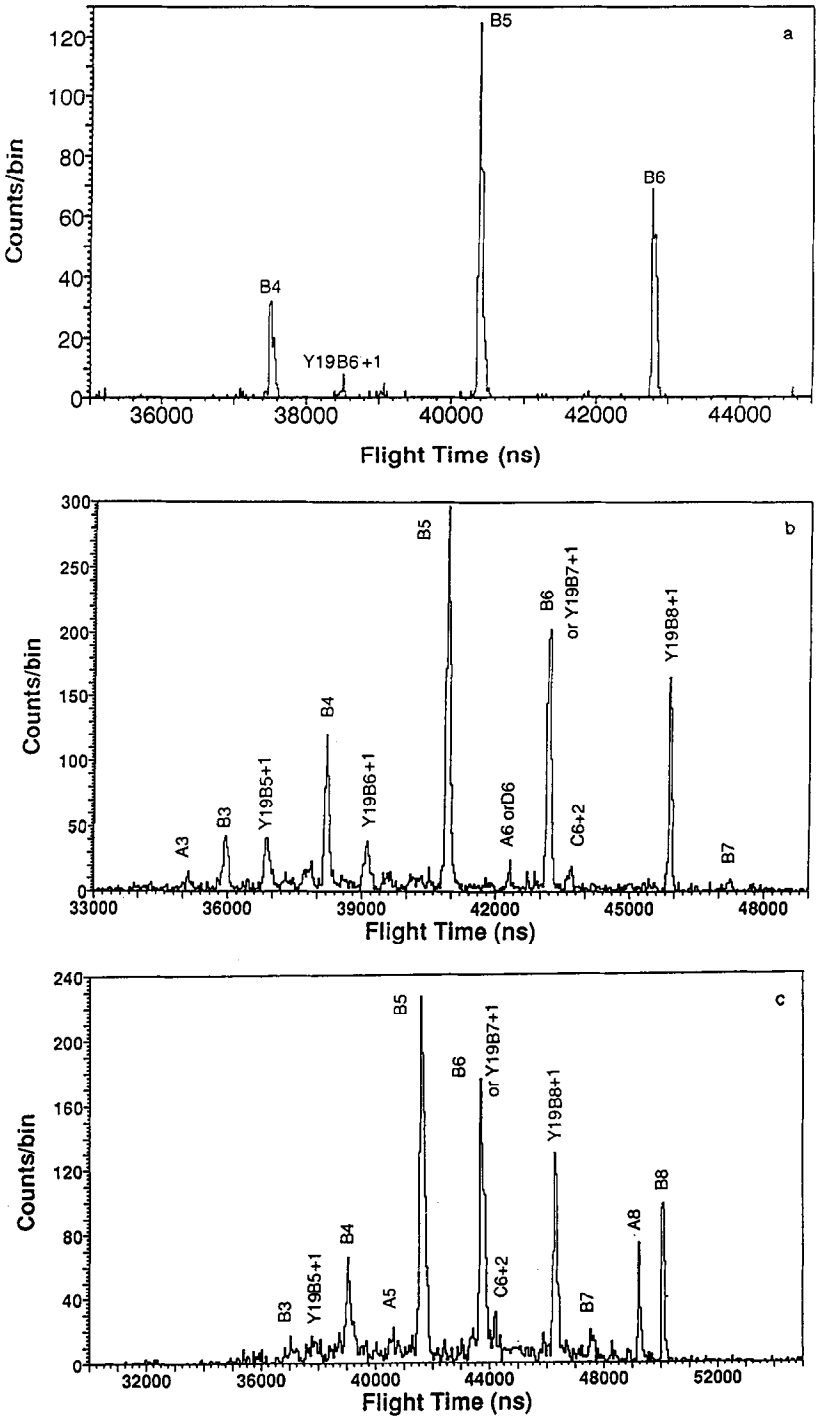

Fig. 9. Daughter ion spectra of (a) B_7, (b) B_8 and (c) B_9 parent ions.

coincides with the flight time observed previously for its parent [20,23]. The mirror then provides full correction for the velocity spread of the daughter, instead of the partial correction when the mirror is optimized for the parent. Under this condition, $m_p/V_p = m_1/V_1 = m_2/V_2$ where m_p, m_1 and m_2 are the masses of the parent and the two daughter ions, and V_p, V_1 and V_2 are the corresponding mirror voltages [19]. The procedure yielded well-resolved isotopic peaks for the selected daughter and enabled residue 18 to be determined as Gln/Lys within an error $\lesssim 0.1$ u by measurement of the principal masses. Resolution of the other peaks was also improved, defining residue 16 as Aib.

The Gln/Lys ambiguity is not easy to resolve by mass measurements, since the mass difference is only about 0.04 u. N-acetylation is an effective method that we have used previously in another case [28]. Here, however, the presence of basic residues near the C terminus would give strong C-terminal ions instead of the B ions observed, so residues 18 and 19 cannot be Gln. Thus the upper part of the sequence is defined as Aib_{16}–Aib_{17}–Gln_{18}–Gln_{19}–Phe_{20}–ol in accordance with the structure suggested by the NMR measurements.

(*d*) *Anomalous isotopic ratios*

As mentioned above, residue 18 was determined to be Gln by measurements of the principal masses. However, some anomalies were noticed in the spectra with unit mass resolution, e.g. the $[M + Na]^+$ peak of Fig. 7, and the daughter ion spectra just described. For example, the $Y_7 + 2$ daughter of the $[M + H]^+$ ion has well resolved peaks whose relative heights ($100 : \approx 90 : \approx 55$) differ from the expected ratios of (100 : 46 : 11), consistent with the presence of an impurity 1 u greater in mass. Here the well-resolved spectra bracketing residue 18 are definitive; the $Y_7B_{17} + 1$ peak heights agree with the expected isotopic ratios (100 : 22 : 3), but those of $Y_7B_{18} + 1$ do not. The ratios for $Y_7B_{19} + 1$ are similar to those for $Y_7B_{18} + 1$, so the impurity is not in residue 19. Thus the sample must contain an impurity with Glu instead of Gln at position 18, i.e. alamethicin I. Indeed, when the sample was rechromatographed, an impurity peak consistent with alamethicin I was resolved. It was also observed that the isotopic ratios became even more anomalous after the sample had been stored in a frost-free freezer for a long time.

(*e*) *Other alamethicins*

Some other HPLC fractions of the alamethicin preparation (Table 2) were examined in a similar, but much more cursory fashion [30]. In all cases, the spectra showed similar characteristics: the first 14 amino acids were relatively easy to determine, the remainder being more difficult; a good deal of metastable decay occurred; the protonated molecular ion was of low abundance; the peak for the sodiated peptide was usually adequate for molecular weight determination. In some cases, the mass uncertainty was considerable as a result of extensive metastable decay. The collected HPLC fractions all contained more than one peptide, often due to contamination from neighboring fractions, and were examined in that form.

The compounds observed result from interchange of various amino acid residues, as expected from the measurements on alamethicins prepared by traditional methods [10]. The major components arise from combinations of the variations $Ala_4 \leftrightarrow Aib_4$ (14 u) and/or $Aib_5 \leftrightarrow Val_5$ (14 u), $Ala_6 \leftrightarrow Aib_6$ (14 u), $Aib_{17} \leftrightarrow Val_{17}$ (14 u), and $Gln_{18} \leftrightarrow Glu_{18}$ (1 u). For the 14 u interchanges, correlation spectra show clearly both the mass change and the location of the modification, as illustrated in Fig. 11. For the Gln ↔ Glu interchanges, no spectra at reduced mirror voltages were examined, so the 1 u difference was discernible mainly in the anomalous isotopic peak height ratios of $[M + Na]^+$. Also, the

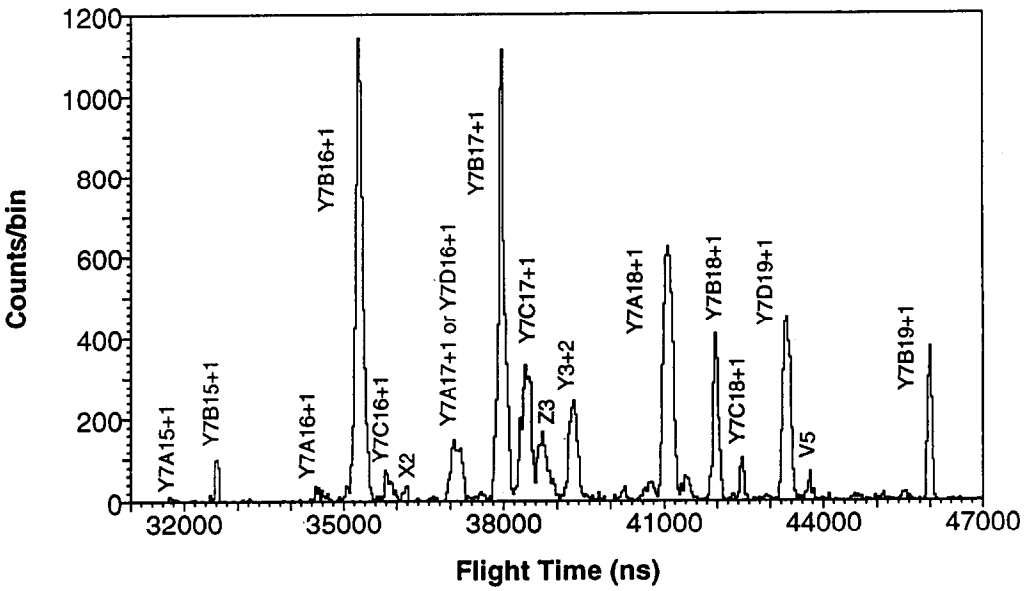

Fig. 10. Daughter ion spectrum of $Y_7 + 2$ parent ions.

molecular ions in the negative ion spectra seemed to be 1 u higher than expected from the positive ion spectra, perhaps due to the presence of small amounts of peptides containing Glu_{18} (which would be expected to produce $[M - H]^-$ ions much more readily than a peptide containing Gln_{18}). These data were sufficient to determine that both were usually present.

The sequences proposed in Table 2 show some agreement with previous GC/MS data [10] for alamethicins prepared by traditional methods, as expected.

4. Discussion

4.1. Sequence determination

Observation of the daughter ions from decay of the $[M + H]^+$ ion is sufficient in principle to define the sequence, provided that the peak assignments are correct. In practice, however, some of the daughter ions may be absent, or of too low intensity. In Fig. 8 the only B ions strong enough to give good measurements are B_8 to B_{13}. It is therefore necessary to observe also the decay of a number of prompt fragments. The $Y_7 + 2$ ion is particularly important in this case, since it is the only intense parent (besides $[M + H]^+$) covering the C-terminal region of the peptide.

A unique assignment for a daughter is not always possible in a given spectrum so it is helpful to have various daughter ion spectra available. This is especially true in alamethicin because of the large number of identical residues; ambiguous peaks are marked with asterisks in Table 1. These overlaps are often between B ions and various internal fragments [30]. Because the internal fragment ions formed usually depend on the parent ion, different parents tend to have different overlaps occurring in their daughter ion spectra, so that there is usually at least one correlation spectrum in which a particular ion peak is unambiguous. For example, the B_3 daughter ion appears in eight different correlation spectra. It overlaps with other ions in the daughter spectra of B_7 ($X_{16}B_7 + 1$), B_9

Table 1
Metastable decay

		Parent ion, B_n →											
	Daughter ion	B_{14}	B_{13}	B_{12}	B_{11}	B_{10}	B_9	B_8*	B_7	B_6*	B_5	B_4	B_3	B_2
(a) Losses from the C terminus of B_n	B_{13}													
	B_{12}													
	B_{11}		0.1*											
	B_{10}	1*	0.8	0.3*										
	B_9	0.3*	0.5	0.3	0.1									
	B_8	0.8*	1	1*	1	0.5	0.3							
	B_7		0.1			0.1	0.1							
	B_6*	0.2*	0.6*	0.5*	0.6*	0.7*	0.7*	0.6*	0.7*					
	B_5	0.3*	0.7*	0.6*	0.5	1*	1*	1*	1*	0.6				
	B_4		0.3	0.3*	0.1	0.1*	0.4*	0.5	0.5*	1	1			
	B_3		0.1	0.1*			0.1*	0.3	0.1*	0.8	0.7	1		
	B_2									0.1	0.1*	0.2	1	
(b) Losses from the C terminus plus cleavage at Aib_1–Pro_2[a]	$Y_{19}B_{13}$*													
	$Y_{19}B_{12}$													
	$Y_{19}B_{11}$*		0.1*											
	$Y_{19}B_{10}$*		0.2*	0.2*	0.1*	0.1								
	$Y_{19}B_9$*		0.1*	0.1*	0.1*	0.1*	0.1*							
	$Y_{19}B_8$	0.1*	0.2	0.4*	0.2	0.3*	0.5*	0.3						
	$Y_{19}B_7$*	0.2*	0.6*	0.5*	0.6*	0.7*	0.7*	0.6*	0.7*					
	$Y_{19}B_6$					0.1	0.1*	0.2	0.1	0.5				
	$Y_{19}B_5$					0.1	0.2*	0.3		0.8*	0.6			
	$Y_{19}B_4$									0.8*	0.4	0.9		
	$Y_{19}B_3$									0.1*		0.1*	0.2	

For peaks marked with an asterisk the intensity reported may be partially or wholly due to overlap of this peak with another one. In general[a], $B_6 \approx Y_{19}B_7$; $B_8 \approx Y_7B_{20}$; $Y_{19}B_9 \approx A_8 \approx D_8$; $Y_{19}B_{10} \approx D_9$; $Y_{19}B_{11} \approx C_9 + 2$; $Y_{19}B_{13} \approx A_{12}$. B_6 and B_8 are more likely than the alternatives. (Note that this overlap also occurs for parent B_6 and B_8 ions.) The other overlaps shown are specific to a particular parent[a]: B_4 daughters, $Y_{19}B_3 \approx X_{18}B_4$; B_5 daughters, $B_2 \approx V_{18}B_5 \approx W_{18}B_5$; B_6 daughters, $Y_{19}B_3 \approx X_{16}B_6$, $Y_{19}B_4 \approx X_{17}B_6$, $Y_{19}B_5 \approx X_{18}B_6$; B_7 daughters, $B_3 \approx X_{16}B_7$, $B_4 \approx X_{17}B_7$, $B_5 \approx X_{18}B_7$; B_8 daughters, $B_5 \approx X_{17}B_8$; B_9 daughters, $B_3 \approx Y_{14}B_9$, $B_4 \approx Y_{15}B_9$, $B_5 \approx Y_{16}B_9$, $B_6 \approx Y_{17}B_9 \approx Y_{19}B_7$, $Y_{19}B_5 \approx X_{14}B_9$, $Y_{19}B_6 \approx X_{15}B_9$, $Y_{19}B_8 \approx Y_{18}B_9$; B_{10} daughters, $B_4 \approx Z_{14}B_{10}$, $B_6 \approx Z_{16}B_{10} \approx V_{16}B_{10} \approx W_{16}B_{10} \approx Y_{19}B_7$, $B_5 \approx Y_{15}B_{10}$, $Y_{19}B_8 \approx Y_{17}B_{10}$; B_{12} daughters, $B_3 \approx V_{12}B_{12}$, $B_4 \approx X_{12}B_{12}$, $B_5 \approx X_{13}B_{12}$, $B_8 \approx X_{16}B_{12}$, $B_{10} \approx V_{19}B_{12} \approx W_{19}B_{12}$, $Y_{19}B_8 \approx Z_{15}B_{12} \approx V_{15}B_{12} \approx W_{15}B_{12}$; B_{13} daughters, $B_5 \approx X_{12}B_{13}$, $B_{11} \approx X_{18}B_{13}$. Note that because B_n and Y_mB_n ions predominate, the other ions mentioned are less likely.

[a] Internal fragment ions appear with an addition proton, e.g. $Y_{19}B_n + 1$.

($Y_{14}B_9 + 1$), and B_{12} ($V_{12}B_{12} + 1$). Although some of these alternative assignments may be unlikely, it is reassuring to have five other spectra where B_3 is clearly assigned. Another example is the B_5 daughter that appears in nine different correlation spectra, in four of them as the major peak. In six cases there is some ambiguity, but in three the daughter B_5 is clearly assigned.

Ambiguities may also arise in parent ion assignment. B_6 and the internal fragment $Y_{19}B_7 + 1$ differ in mass by only 1 u, so both can be included in the same peak in the neutral spectrum. Most of the ≈ 20 daughter ion peaks could originate from either parent, but three can only come from B_6 and a different three only from $Y_{19}B_7 + 1$. Therefore both parent ions must be present.

The redundancy provided by measurements of daughter ions from a large set of parents, as in Table 1, thus leads to more accurate mass measurements and increased confidence in the assignments. The usual measurements may leave some uncertainty where possible residues

Table 2
HPLC fractions of alamethicin preparation

HPLC fraction (min)	Principal mass (u)[a]	Variations from alamethicin III (in bold type)							Principal mass (from sequence)[b]	Assignment[c]
21.34	1962 ± 0.5 (la)	...Ala_4	Aib_5	Ala_6	Gln_7...Aib_{16}	Aib_{17}	Gln_{18}	Gln_{19}...	**1962.1**	**alam III**
	1963 ± 0.5 (m)	...Ala_4	Aib_5	Ala_6	Gln_7...Aib_{16}	Aib_{17}	**Glu_{18}**	Gln_{19}...	1963.1	alam I
	1976 ± 2 (sm)	... ?	...							
22.56	1962.5 ± 1.5 (m)	...Ala_4	Aib_5	Ala_6	Gln_7...Aib_{16}	Aib_{17}	Gln_{18}	Gln_{19}...	1962.1	alam III
		...Ala_4	Aib_5	Ala_6	Gln_7...Aib_{16}	Aib_{17}	**Glu_{18}**	Gln_{19}...	1963.1	alam I
	1976.8 ± 1.5 (la)	...Ala_4	Aib_5	Ala_6	Gln_7...Aib_{16}	**Val_{17}**	Gln_{18}	Gln_{19}...	**1976.2**	**alam IV**
		...Ala_4	Aib_5	Ala_6	Gln_7...Aib_{16}	**Val_{17}**	**Glu_{18}**	Gln_{19}...	**1977.1**	**alam V**
	1992 ± 3 (sm)	...Ala_4	Aib_5	**Aib_6**	Gln_7...Aib_{16}	**Val_{17}**	Gln_{18}	Gln_{19}...	1990.2	alam VI
		...Ala_4	Aib_5	**Aib_6**	Gln_7...Aib_{16}	**Val_{17}**	**Glu_{18}**	Gln_{19}...	1991.2	alam VII
23.33	1962.8 ± 0.5 (la)	...Ala_4	Aib_5	Ala_6	Gln_7...Aib_{16}	Aib_{17}	**Glu_{18}**	Gln_{19}...	**1963.1**	**alam I**
	1975.9 ± 0.5 (la)	...Ala_4	Aib_5	**Aib_6**	Gln_7...Aib_{16}	Aib_{17}	Gln_{18}	Gln_{19}...	**1976.2**	**alam VIII**
		...Ala_4	Aib_5	**Aib_6**	Gln_7...Aib_{16}	Aib_{17}	**Glu_{18}**	Gln_{19}...	1977.1	alam II
24.53	1963.5 ± 1.5 (sm)	...Ala_4	Aib_5	Ala_6	Gln_7...Aib_{16}	Aib_{17}	**Glu_{18}**	Gln_{19}...	1963.1	alam I
	1977.2 ± 1 (la)	...Ala_4	Aib_5	**Aib_6**	Gln_7...Aib_{16}	Aib_{17}	Gln_{18}	Gln_{19}...	**1976.2**	**alam VIII**
		...Ala_4	Aib_5	**Aib_6**	Gln_7...Aib_{16}	Aib_{17}	**Glu_{18}**	Gln_{19}...	**1977.1**	**alam II**
	1990.4 ± 1.5 (la)	...Ala_4	Aib_5	**Aib_6**	Gln_7...Aib_{16}	**Val_{17}**	Gln_{18}	Gln_{19}...	**1990.2**	**alam IX**
		...Ala_4	Aib_5	**Aib_6**	Gln_7...Aib_{16}	**Val_{17}**	**Glu_{18}**	Gln_{19}...	**1991.2**	**alam X**
25.57	1961.3 ± 1.5 (sm)	...Ala_4	Aib_5	Ala_6	Gln_7...Aib_{16}	Aib_{17}	Gln_{18}	Gln_{19}...	1962.1	alam III
		...Ala_4	Aib_5	Ala_6	Gln_7...Aib_{16}	Aib_{17}	**Glu_{18}**	Gln_{19}...	1963.1	alam I
	1977.1 ± 1.5 (la)	...Ala_4	Aib_5	**Aib_6**	Gln_7...Aib_{16}	Aib_{17}	Gln_{18}	Gln_{19}...	1976.2	alam VIII
		...Ala_4	Aib_5	**Aib_6**	Gln_7...Aib_{16}	Aib_{17}	**Glu_{18}**	Gln_{19}...[d]	**1977.1**	**alam II**
		...Ala_4	**Val_5**	Ala_6	Gln_7...Aib_{16}	Aib_{17}	Gln_{18}	Gln_{19}...[e]	1976.2	alam XI
		...Ala_4	**Val_5**	Ala_6	Gln_7...Aib_{16}	Aib_{17}	**Glu_{18}**	Gln_{19}...[e]	1977.1	alam XII
		...**Aib_4**	Aib_5	Ala_6	Gln_7...Aib_{16}	Aib_{17}	Gln_{18}	Gln_{19}...[e]	1976.2	alam XIII
		...**Aib_4**	Aib_5	Ala_6	Gln_7...Aib_{16}	Aib_{17}	**Glu_{18}**	Gln_{19}...[e]	1977.1	alam XIV

[a] (la) represents a large peak, (m) a medium sized peak, and (sm) a small peak.

[b] The major peptide is in bold face; minor ones are in standard type. If no choice can be made between peptides for a given mass peak, or if both are equally present, both are in the same type.

[c] Alamethicin I and II were previously numbered; the other alamethicins are numbered in order of HPLC elution; it is not known how these numbers relate to those of Brewer et al. [14]; alam = alamethicin.

[d] Note that for the 25.57 min fraction, 1977.1 u, Aib_6Glu_{18} is preferable to Aib_6Gln_{18} because of the peak height ratios and the mass.

[e] These are presented by such small peaks that they cannot be differentiated. The Aib_4 version seems more likely than the Val_5 version.

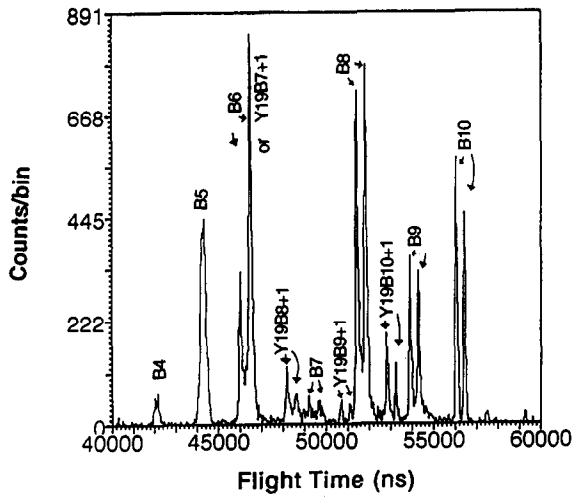

Fig. 11. Daughter ion spectrum of B_{13} parent ions of the 23.33 min fraction of alamethicin. Up to position five the peaks are single and from position six on they are double, showing that two different amino acids are present at position six.

differ by only one or two units, but such problems can be solved by bracketing the uncertain residue, as seen for the Glu_{18}/Gln_{18} case above, and impurity levels can be estimated, even for mass differences of 1 u.

4.2. Decay pattern

A major part of all spectra consists of B_n ions, along with some of the complementary $Y_m + 2$ ions, particularly the complementary pair $B_{13}/Y_7 + 2$. B_n ions are commonly found in peptides without basic residues, such as alamethicin III. Formation of B_n and $Y_m + 2$ ions for such peptides may be initiated by protonation at amide nitrogens [34].

It is clear that cleavage at Aib–Pro is favored in the alamethicins, especially from the intensity of the $B_{13}/Y_7 + 2$ pair of ions. The abundant internal fragment series $Y_{19}B_n + 1$ and $Y_7B_n + 1$ also correspond to cleavage at Pro_2 and Pro_{14} respectively. Similar behavior is observed in studies of other peptides containing Aib–Pro bonds [1,11], and analogous effects are observed in some charged peptides [29,34] and in nonbasic bradykinin derivatives [35].

Measurements have shown that the proton affinity of Pro is exceeded only by Arg, Lys, and Glu [36], and perhaps Gln [36,36(a)]. None of the first three is represented in alamethicin III. Neglecting the uncertain Gln, and because acetylation has reduced the Proton affinity of the N terminus, it might be argued that the charge is quite likely to reside on the amide nitrogen of Pro, leading to the observed cleavages. As mentioned above, however, basic peptides (i.e. those containing Arg and Lys) may also exhibit large amounts of cleavage at Pro, so proton affinities cannot be the only explanation for the lability of the bond. As discussed by Loo et al. [13(a)], the behaviour seems to be related to the great stability of peptide fragments containing Pro at the N terminus [13(a)]. It may also be related to conformational changes induced by Pro [13(a)]; such changes have been observed in the alamethicins [37] and are common.

The wealth of data accumulated allows some observations regarding the metastable decay of alamethicin and its prompt fragments. It is interesting to note that the direct spectrum peaks in Fig. 4a represent the total amount of each fragment ion produced (i.e. both the metastable decay products and the ions that reach the detector intact), although the peak intensities may also reflect some mass dependence of the detector efficiency of the microchannel plate detectors. The neutral peaks shown in Fig. 4b represent the amount of each prompt parent ion decaying, since they represent neutral daughters reaching detector 1 when the ion mirror field is on (Fig. 2). As is evident from Fig. 4, A_1 and B_1 exhibit less decay than average (probably because they contain no peptide bonds), and B_2 and $Y_7 + 2$ show more metastable decay than the rest of the fragments. The unusual susceptibility of B_2 to metastable decay confirms that the Aib–Pro bond is labile in the gas phase ion

as well as during desorption/ionization and in solution chemistry. This is also shown by the internal fragment daughter ion series appearing in many of the correlation spectra.

As mentioned, the alamethicins have an anomalously large extent of metastable decay in the flight tube. We also observed such decay for synthetic alamethicin in which Ala replaces all of the Aib residues and a carboxylic acid at the C terminus replaces the alcohol. The data demonstrate that neither the Aib residues nor the terminal alcohol seems to be responsible for the short lifetime of these molecules. From previous work on alamethicin I and II [5–7], it seems that the peptides containing Glu instead of Gln show the same behavior. Thus the neutrality of the peptide does not seem to have an effect. However, the lack of basic residues in the peptide and the lack of a basic NH_2 at the N terminus seems to be significant.

4.3. The correlation method

The principal advantage of the present method is seen in the large amount of data — all of the correlation spectra as well as the neutral and direct spectra — produced in a single experimental run. Since all daughter ions are produced at the same time, problems of normalization are minimized and the overall decay pattern shows up clearly. The redundancy provided is a considerable help in sequence determination.

A related advantage is the increased sensitivity inherent in the TOF correlation technique. Unlike in other spectrometers, ions are not lost when they decay, but can be used to obtain sequence information. The only scanning ever needed involves reducing the mirror voltage, and this is not usually necessary. Although about 5 nmol of sample were used on a target purely for convenience, we have previously reported [24(a)] that this technique is capable of giving almost complete daughter ion spectra from samples of about 200 fmol. However, if the smaller sample reduced the number of ions produced, we would have had to increase the primary ion current or else take data for a longer time.

We note that tandem measurements of the similar trichosporin compounds with a triple quadrupole mass spectrometer required examination of the decay of ions analogous to ours in separate measurements, particularly the $Y_7 + 2$ ion [11]. Resolution in these measurements was better than ours, but it appears that a wider and more useful variety of ions was produced in our technique.

A disadvantage is the limited resolution obtained for the parent ions ($M/\Delta M < 100$ here). This value is considerably lower than the resolution of MS-1 in most tandem spectrometers. Similar values to ours have been reported for TOF instruments where the parent ions are selected by opening a gate between the acceleration region and the mirror [38,39], so the limit is not imposed by the correlation method; rather it is a result of selecting the parent in a linear TOF spectrometer. It may be possible to do better in a tandem TOF instrument where parent ions are selected after reflection [40,41].

A second disadvantage is the large amount of time required for a run — several hours in general. Here there is an intrinsic limitation specific to the correlation technique; the overall counting rate must be limited to less than one correlated pair per pulse in order to define the correlated particle uniquely. (This also precludes the use of the method for ions produced by matrix assisted laser desorption/ionization.) However, the practical limitation at present is the speed of the data system, which restricts the counting rate to $\leqslant 4000$ events s^{-1}. Consequently, the pulse repetition rate is limited to 4 kHz. In principle, this repetition rate is limited only by the longest flight time of interest. Recent improvements allow

accelerating voltages up to 30 kV, and therefore shorter flight time, permitting a pulse repetition rate of 20 kHz. Thus an improvement in counting rate by a factor of about 5 is expected with a faster data system, now under development; further improvements may be possible.

5. Conclusion

Alamethicin III, like the two alamethicins known previously, has eight α-aminoisobutyric acid residues, an acetyl group at the N terminus, and a phenylalaninol at the C terminus. It has neither acidic nor basic residues, unlike alamethicins I and II which have an acidic residue. Its sequence, as deduced from our mass measurements, is

$Ac–Aib_1–Pro_2–Aib_3–Ala_4–Aib_5–Ala_6–$
$Gln_7–Aib_8–Val_9–Aib_{10}–Gly_{11}–(Leu/Ile)_{12}–$
$Aib_{13}–Pro_{14}–Val_{15}–Aib_{16}–Aib_{17}–Gln_{18}–$
$Gln_{19}–Phe_{20}–ol$

This sequence agrees with the NMR data, which also reveal that residue 12 is Leu. Sequences are proposed for a number of the minor components of the mixture produced by the fungus (see Table 2). In addition, the data yielded by the TOF correlation technique have given an improved understanding of the fragmentation processes taking place in these compounds.

Acknowledgments

We thank Alan Hyland for his assistance. This research was supported by the US National Institutes of Health (GM30605) and by the Natural Sciences and Engineering Research Council of Canada. N.P.-S. acknowledges the support of the Manitoba Health Research Council.

Appendix 1: Decay in the acceleration region

In the simplest case, a parent ion P^+ is produced at the target and is accelerated across a potential difference V applied between the target and a grounded grid at a distance L from the target, reaching a kinetic energy $T_p = 1/(2m_p v_p^2) = q_p V$. The parent ion P^+ then decays in free flight between the grid and the ion mirror to give charged and neutral daughters ($P^+ \rightarrow D^+ + N$). For simplicity assume zero energy release in the disintegration; then both daughters retain the velocity of the parent ion, and the time of arrival of the neutral daughter at detector 1 defines the parent ion mass m_p.

If the decay occurs in the acceleration region instead of in free flight, the neutral daughter will have a velocity different from the reference value above, so it will simply produce background between the peaks corresponding to various parent ions. However, these peaks have an appreciable breadth resulting from the energy release in the decay (and from the effect considered here), so some neutral daughters from decays in the acceleration region will still be included. Two cases are of particular interest:

1. Where the decay of P^+ occurs just inside the grid, i.e. at distance x from the target where $(L - x)/L \ll 1$. In this case,

$$T_p = mv_p^2/2 = q_p V x/L$$

$$\Delta T_p/T_p = (T_p - T_p)/T_p = (x/L) - 1$$

$$\text{Time spread } \Delta t/t = -\Delta T_p/2T_p$$

$$= [1 - (x/L)]/2$$

2. Where the parent ion P^+ is itself produced by the decay of a predecessor α^+ close to the target, i.e. at distance x, where $x/L \ll 1$. In this

case,

$T_p = mv_p^2/2 = q_p V[(L-x)/L + xm_p/Lm_\alpha]$

$\Delta T_p/T_p = -x(1-(m_p/m_\alpha)]/L$

Time spread $\Delta t/t = x[1-(m_p/m_\alpha)]/2L$

In the present experimental configuration the acceleration distance L is 0.9 cm, the distance between grid and mirror is 50 cm, and the acceleration voltage V is 10 kV. The flight time of the $(M+H)^+$ ion is then $\approx 16\,\mu s$ between grid and mirror, and ≈ 570 ns in the acceleration region.

For case 1 if we assume an acceptable time spread $\Delta t/t = 0.01$, decays in the distance from $x/L = 0.98$ to $x/L = 1$ will give neutrals in the defining peak. This corresponds to a time interval for the decay of only 6 ns (time interval $= 570 - 570(0.98)^{1/2} \approx 6$ ns), so the contribution of this process to the peak is unlikely to be significant.

Case 2 gives a much larger effect. Again assuming $\Delta t/t = 0.01$, neutrals appear in the defining peak if the first decay takes place within a distance x from the target, where $x/L = 0.02/[1-(m_p/m_\alpha)]$, which is larger than the value for case 1. More important, the ion is just starting its motion, so the corresponding time interval for the decay (if the neutrals are to appear in the defining peak) is much longer. Also, any ion which decays close to the target has a very high decay rate (assuming exponential decay) so many ions are involved and the effect is magnified.

e.g. for $\alpha^+ = [M+H]^+$ and $P^+ = B_{13}$

$x/L \approx 0.02/[1-(12/20)] = 0.05$

Time interval $= 570(0.05)^{1/2} \approx 127$ ns

e.g. for $\alpha^+ = [M+H]^+$ and $P^+ = Y_7 + 2$

$x/L \approx 0.02/[1-(7/20)] = 0.4/13 \approx 0.03$

Time interval $= 570(0.4/13)^{1/2} \approx 100$ ns

Although these times are small compared to the overall flight time, the contribution from this process (case 2) may be large when the precursor ion α^+ has a short lifetime, as appears to be the situation in alamethicin. The resulting peak is broadened towards longer flight time, giving a possible systematic error in mass determination, i.e. a mass larger than it should be.

There will be corresponding changes in the energy of the charged fragment also, but these will be corrected by the mirror, at least partially, so normally they are less significant.

References

[1] H. Brückner and M. Przybilski, J. Chromatogr., 296 (1984) 263.

[2] H.T. Tien, Bilayer Lipid Membranes (BLM): Theory and Practice, Marcel Dekker, New York, 1974.

[3] M. Eisenberg, J.E. Hall and C.A. Mead, J. Membr. Biol., 14 (1973) 143.

[4] T. Fujita, Y. Takaishi, K. Matsuura, Y. Takeda, Y. Yoshioka and H. Brückner, Chem. Pharm. Bull., 32 (1984) 2870.

[5] R.C. Pandey, H. Meng, J.C. Cook, Jr., and K.L. Rinehart, Jr., J. Am. Chem. Soc., 99 (1977) 5205.

[6] R.C. Pandey, J.C. Cook, Jr., and K.L. Rinehart, Jr., J. Am. Chem. Soc., 99 (1977) 8469.

[7] B.T. Chait, B.F. Gisin and F.H. Field, J. Am. Chem. Soc., 104 (1982) 5157.

[8] D.R. Martin and R.J.P. Williams, Biochem. J., 153 (1976) 181.

[9] T.M. Balasubramanian, N.C.E. Kendrick, M. Taylor, G.R. Marshall, J.E. Hall, I. Vodayanoy and F. Reusser, J. Am. Chem. Soc., 103 (1981) 6127.

[10] W.A. König and M. Ayden, in K. Brunfeldt (Ed.), Peptides, Proceedings of the 16th European Peptide Symposium, Scriptor, Copenhagen, 1980, p. 711.

[11] A. Iida, M. Okuda, S. Uesato, Y. Takaishi, T. Shigu, M. Morita and T. Fujita, J. Chem. Soc., Perkin Trans. 1, (1990) 3249.

[12] The Upjohn Company, UK Patent 1 152 659, 1966.

[13] M. Przybylski, I. Dietrich, I. Manz and H. Brückner, Biomed. Mass Spectrom., 11 (1984) 569.

[13] (a) J.A. Loo, C.G. Edmonds and R.D. Smith, Anal. Chem., 65 (1993) 425.

[14] D. Brewer, F.G. Mason and A. Taylor, Can. J. Microbiol., 33 (1987) 619.

[15] A. Yee and J. O'Neil, Biochemistry, 31 (1992) 3135.

[16] S. Della-Negra and Y. LeBeyec, Int. J. Mass Spectrom. Ion Processes, 61 (1984) 21; Anal. Chem., 57 (1985) 2035; Springer Proc. Phys., 9 (1986) 42.

[17] K.G. Standing, W. Ens, R. Beavis, G. Bolbach, D. Main,

B. Schueler and J.B. Westmore, Springer Proc. Phys., 9 (1986) 37.
[18] X. Tang, W. Ens, K.G. Standing and J.B. Westmore, Anal. Chem., 60 (1988) 1791.
[19] X. Tang, R. Beavis, W. Ens, F. Lafortune, B. Schueler and K.G. Standing, Int. J. Mass Spectrom. Ion Processes, 85 (1988) 43.
[20] K.G. Standing, W. Ens, F. Mayer, X. Tang and J.B. Westmore, in A. Hedin, B.U.R. Sundquist and A.B. Benninghoven (Eds.), Ion Formation from Organic Solids-IFOS V, Wiley, Chichester, 1990, p. 93.
[21] K.G. Standing, W. Ens, F. Mayer, X. Tang and J.B. Westmore, in E.R. Hilf and W. Tuszynski (Eds.), Mass Spectrometry of Large Non-Volatile Molecules for Marine Organic Chemistry, World Scientific, Singapore, 1990, p. 186.
[22] K.G. Standing, W. Ens, X. Tang and J.B. Westmore, in D. Desiderio (Ed.), Mass Spectrometry of Peptides, CRC Press, Boca Raton, FL, 1990, p. 159.
[23] X. Tang, W. Ens, F. Mayer, K.G. Standing and J.B. Westmore, Rapid Commun. Mass Spectrom., 3 (1989) 443.
[24] X. Tang, Ph.D. Dissertation, University of Manitoba, 1991.
[24] (a) X. Tang, W. Ens and K.G. Standing, Proceedings of the 38th ASMS Conference on Mass Spectrometry and Allied Topics, Tucson, AZ, 1990, p. 542
X. Tang, W. Ens, N. Poppe-Schriemer and K.G. Standing and W. Ens (Eds.), Methods and Mechanisms for Producing Ions from Large Molecules, in the NATO ASI Series, Plenum, New York, 1991, p. 139.
[25] J. Zhou, Ph.D. Dissertation, University of Manitoba, 1994.
[26] W. Ens, K.G. Standing and A. Verentchikov, in G.J. Blanar and R.J. Cotter (Eds.), Proc. Int Conference on Instrumentation for Time-of-Flight Mass Spectrometry, LeCroy Corp., Chestnut Ridge, NY, 1993, p. 137.
[27] K.G. Standing, R. Beavis, W. Ens, X. Tang and J.B. Westmore, in C.J. McNeal (Ed.), The Analysis of Peptides and Proteins by Mass Spectrometry, Wiley, Chichester, 1988, p. 267.
[28] N. Poppe-Schriemer, D.R. Binding, W. Ens, F. Mayer, K.G. Standing and J.B. Westmore, Int. J. Mass Spectrom. Ion Processes, 11 (1991) 301.
[29] S.A. Martin and K. Biemann, Int. J. Mass Spectrom. Ion Processes, 78 (1987) 213.
[30] N. Poppe-Schriemer, Ph.D. Thesis, University of Manitoba, 1995.
[31] J.M. Curtis, P. Thibault, R.K. Boyd, S. Chen, P.J. Derrick and B.A. Thomson, Proc. 41st ASMS Conference on Mass Spectrometry, San Francisco, CA, 1993, pp. 921a–b.
[32] P. Roepstorff and J. Fohlman, Biomed. Mass Spectrom., 11 (1984) 601.
[33] K. Biemann and S.A. Martin, Mass Spectrom. Rev., 6 (1987) 1.
[34] D.F. Hunt, J.R. Yates III, J. Shabanowitz, S. Winston and C.P. Hauer, Proc. Natl. Acad. Sci. USA, 83 (1986) 6233.
[35] D. Bunk and R. Macfarlane, Int. J. Mass Spectrom. Ion Processes, 111 (1991) 55.
[36] G.S. Gorman, J.P. Speir, C.A. Turner and I.J. Amster, J. Am. Chem. Soc., 114 (1992) 3986.
[36] (a) Z. Wu and C. Fenselau, Rapid Commun. Mass Spectrom., 6 (1992) 403.
[37] R.O. Fox and F.M. Richards, Nature, 300 (1982) 325.
[38] R. Kaufmann, B. Spengler and F. Lützenkirchen, Rapid Commun. Mass Spectrom., 7 (1993) 902.
[39] J. Hoyes, S. Curbishely, P. Doorbar, P. Tatterton, R.H. Bateman, B. Beer and J. Lockett, 42nd ASMS Conference on Mass Spectrometry, Chicago, IL, May/June 1994, paper WP9.
[40] T.J. Cornish and R.J. Cotter, Org. Mass Spectrom., 28 (1993) 1129.
[41] M.A. Seeterlin, P.R. Vlaseck, D.J. Beussman, R.D. McLane and C.G. Enke, J. Am. Soc. Mass Spectrom., 4 (1993) 751.